WEB WRINKLING RESULTING FROM MOMENT TRANSFER

Boshen Fu and James K. Good
Oklahoma State University
USA

ABSTRACT

Considerable research has been focused on the impact of roller misalignment on web instability. Early work focused on the prediction of trough instabilities in the entering span, just upstream of the misaligned roller [1]. Later works involving misaligned [2] and tapered [3] rollers proved that the trough instability was a required precursor for the occurrence of wrinkles on the misaligned or tapered roller. The compressive stress required to induce web wrinkles on a roller can be 2 orders of magnitude larger, in the absolute sense, than the compressive stress required to precipitate trough instabilities in a web span. These works [2][3] found the out-of-plane web deformation due to troughs was responsible for creating the larger compressive stresses that would finally result in wrinkles whenever the misalignment or taper became sufficient. The three works referenced thus far all rely upon an assumption that the friction forces between the web and the upstream roller, which separates the entering and pre-entering spans, are sufficient to prevent moment transfer. The lateral deformation of the web in the pre-entering and entering spans as a result of moment transfer has been another focus of web handling research [4][5]. This publication will focus on the impact of moment transfer on web wrinkling. It will be shown that troughs may now occur in both the pre-entering and entering spans. It will also be shown that wrinkles can precipitate on either the misaligned roller or the roller upstream of the misaligned roller. It will be shown that these behaviors can be predicted and the predictions will be validated by test results. It will be shown that as a result of moment transfer the roller misalignment to induce wrinkles can be less than the misalignment required to induce wrinkles when moment transfer does not occur.

DEFINITIONS

A web span which encounters a disturbance such as a misaligned or a tapered roller at the downstream end will be referred to as the *entry span*. There will be a roller at the upstream end of the entry span, which herein will be assumed to be perfect in terms of

alignment and absence of taper in outer radius. The span upstream of the entry span and this roller will be referred to as the *pre-entry span*. If the disturbance is sufficient *trough* instability can be induced which is defined herein as out-of-plane web deformation in web spans. If the disturbance becomes larger the troughs can grow in amplitude and cause *wrinkles* to transgress rollers. The span downstream of the entry span will be referred to as the *exit* span.

INTRODUCTION

Web wrinkling resulting from disturbances, such as roller misalignment, has long been a subject of interest. Studies have focused on the prediction of trough and wrinkle instabilities in the entry span caused by either a misaligned roller [1][2] or a tapered roller [3] at the downstream end of the span. In these single span analyses, the assumption was made that the frictional force generated between the web and rollers was sufficient to confine the lateral deformation of the web to the single (entry) span and spans downstream. With this assumption troughs will be confined to the entry span if the disturbance is sufficient to induce troughs. If the disturbance becomes larger (greater misalignment or taper) web wrinkles will form on the downstream roller which is the disturbance source. In laboratory tests which validated these analyses the roller upstream of the roller providing the disturbance was covered with a coating that provided a high coefficient of friction. In this way the assumptions assumed in analyses were enforced in the laboratory.

Disturbances will cause a moment in the web at the upstream end of the entry span. Only friction forces between the web and the roller at the upstream end of the entry span can isolate the pre-entry span from the disturbance. There is a limit with regard to the moment that can be reacted by the friction forces called the *critical moment*. When the disturbance induces a moment greater than this critical moment, moments and lateral deformation will transfer into the pre-entry span. An analysis based on beam theory was developed [4], which reveals the relationship between the moment developed at the upstream end of the entry span and a disturbance (a misaligned roller) at the downstream end of the entry span. When the moment surpassed the critical moment the analysis went further to predict the moment distribution and lateral deformation in the pre-entering span. This type of analysis is sufficient to explain the behavior of the lateral deformations of the web on a macro scale but does so by enforcing kinematic and kinetic boundary conditions on the elastic axis of the beam that is used to model the web. The contact normal and friction forces between the web and roller cannot be studied using beam models. A computational and experimental study of moment transfer due to downstream misalignment was reported in [5]. In this study Abaqus/Explicit [6] was employed. Membrane elements were used to model the web and the rollers were modeled as rigid analytical surfaces. The contact normal and friction force distributions between the web and rollers were studied during cases of moment transfer due to a downstream misaligned roller. The benefit of this type of analysis is that only very basic assumptions are required, such as web velocity and web tension, which makes the Abaqus/Explicit simulations show much promise for studying the web handling problems regarding contact forces. The kinematic and kinetic boundary conditions enforced by the previous study [4] were not applied. The frictional contact between the web and rollers in the Abaqus/Explicit simulations now dictate the lateral behavior of the web. The simulation results were used to investigate potential boundary conditions for a broad range of misalignment starting at low levels where moment was not transferring into the pre-entry span and ending in cases where substantial moments were transferred [5]. In the current

study, Abaqus/Explicit will be used to explore web instability and model wrinkle formation in successive web spans due to roller misalignment.

The compressive stress required to wrinkle a web on a roller can be two orders of magnitude larger than that required to induce troughs in a web in a span. The wavelength of a wrinkle is much smaller compared to that of a trough. Large mesh densities are required to capture the small wavelength instability of a wrinkle. Thus simulations of wrinkles are computationally expensive compared to simulations of web troughs in Abaqus/Explicit. To address this issue an efficient modeling technique was developed. A wrinkle failure criterion was employed in previous analyses [2][3] to determine the cross machine direction (CMD) stress required to wrinkle a web on a roller. Use of this criterion was validated in those works by comparison of predictions with test results. Abaqus/Explicit is a fully nonlinear code and can be used to study instability phenomena. In this investigation computational expense was saved by using the previously developed wrinkle criterion. Instead of requiring the mesh density to be sufficient to capture the wavelength of a wrinkle the mesh density was increased only until there was convergence in the stresses. If compressive CMD stresses developed that were more negative than the failure criterion, wrinkling was assumed to have occurred. This yields a large savings in computational time. In this study, the analysis methods and failure criterion will be validated using experimental results. The results will be used to investigate web wrinkles in conditions where moment transfer is present.

THE WRINKLE FAILURE CRITERION

Timoshenko's buckling equation for a cylindrical shell has been used as a failure criterion to develop a closed form solution for wrinkles due to web twist [7], wrinkles due to the effect of roller taper [3] and for wrinkles due to roller misalignment [2] using finite element simulations. In these works Timoshenko's buckling expression was used to calculate the critical compressive stress for a sector of a cylindrical shell subject to axial compression. Then a method was developed that allows the CMD compressive stress in the web on the roller to be predicted as a function of the disturbance level. The disturbance could be twist of the web, taper in roller radius with respect to the CMD or the misalignment of a roller. When the disturbance produces CMD compressive stresses more negative than Timoshenko's expression, a wrinkle instability has occurred in the web on a roller. The buckling expression and length of half-waves for a cylindrical shell developed by Timoshenko [8] are:

$$\sigma_{cr} = \frac{-Et}{R\sqrt{3(1-\nu^2)}} \qquad \{1\}$$

$$\lambda_{cr} = \pi\sqrt[4]{\frac{R^2t^2}{12(1-\upsilon^2)}} \approx 1.72\sqrt{Rt} \qquad \{2\}$$

where E is Young's modulus and ν is Poisson's ratio of the web material, t is the web thickness, R is the radius of the roller. These expressions {1} and {2} were developed for linear homogenous elastic materials. The theory on elastic and plastic buckling of isotropic and anisotropic shells has been well established [9] in recent years. Hence expressions {1} and {2} could be written as more general forms:

$$\sigma_{cr} = \sqrt{\frac{C_{11}C_{22} - C_{12}C_{21}}{3}}\left(\frac{t}{R}\right) \qquad \{3\}$$

$$\lambda_{cr} = \pi\sqrt[4]{\frac{C_{11}^2}{12(C_{11}C_{22} - C_{12}C_{21})}}(Rt)^{1/2} \qquad \{4\}$$

$$\begin{bmatrix}\sigma_x \\ \sigma_y\end{bmatrix} = \begin{bmatrix}C_{11} & C_{12} \\ C_{21} & C_{22}\end{bmatrix}\begin{bmatrix}\varepsilon_x \\ \varepsilon_y\end{bmatrix} \qquad \{5\}$$

In expressions {3-5} the x and y directions are the MD and CMD directions, respectively. It is evident that the critical stress and the length of the half-waves are related to the constitutive expression {5} of the web material in expressions {3} and {4}. If the material is linear elastic, expressions {3} and {4} will reduce to Timoshenko's classic expressions {1} and {2}. Now the web properties can be linear/nonlinear elastic, isotropic/anisotropic, or plastic in behavior as long as the *C* components in the constitutive expression {5} are known. A similar general form expression was developed by Good *et al.* in [10] as well.

For the cases of the a misaligned roller [2], a tapered roller [3], and that of web span twist [7] the CMD compressive stress was calculated where the web was just entering the roller. In each case a means was developed to calculate this stress as a function of the disturbance level. In these cases precise knowledge of the friction forces between the web and roller was not required, only that there was sufficient friction force to sustain a wrinkle on the roller. In the current study of wrinkling associated with moment transfer a new means of calculating these CMD stresses had to be developed. It will be shown that the friction forces between the web and roller associated with moment transfer are responsible for producing the CMD stresses that will result in wrinkling. Abaqus/Explicit simulations have been employed to study these CMD stresses. The stresses will be compared to expression {1} to determine if wrinkling has occurred.

EXPERIMENTAL PROCEDURE AND RESULTS

A schematic of the test setup is shown in Figure 1. In the following discussion the roller R2 separates the pre-entry and entry spans. The roller R3 separates the entry and exit spans. The angle of web wrap for rollers R2 and R3 is $\pi/2$ radians. The lengths of the pre-entry, entry and exit spans were 45.7 cm (18 in), 45.7 cm (18 in) and 88.9 cm (35 in), respectively. The rollers have a nominal diameter of 7.37 cm (2.9 in). Experiments were conducted on an oriented polyester web 23.4 μm (.00092 in) in thickness and 15.24 cm (6 in) in width. The static friction coefficient between the polyester and the bare aluminum roller surfaces is about 0.29 ~ 0.33. Rollers R2 and R3 had rms roughness (R_q) of 0.54 μm (21.3 μin) and 1.91 μm (75.2 μin), respectively. The web velocity was held constant at 15.2 mpm (50 fpm) in all tests. The friction coefficient between rollers R2 and R3 and the web will be affected by entrained air and discussed later. Rollers R1 and R4 had a silicon rubber coating (3M Company[1] 5461) which has a high friction coefficient when in contact with polyester. Tests per ASTM D1894 have shown static friction coefficients in excess of unity. The web was found to be essentially isotropic with a Young's modulus of

[1] 3M Company, 3M Corporate Headquarters, 3M Center, St. Paul, MN 55144-1000, USA.

4 GPa (580,000 psi) and Poisson's ratio of 0.3. The roller R3 was misaligned about an outer normal to the entry span until a wrinkle resulted either on roller R2 or R3. Tests were performed at several web tension levels. For the conditions described, expression {1} yields a critical wrinkling stress of -1.53 MPa (-222 psi).

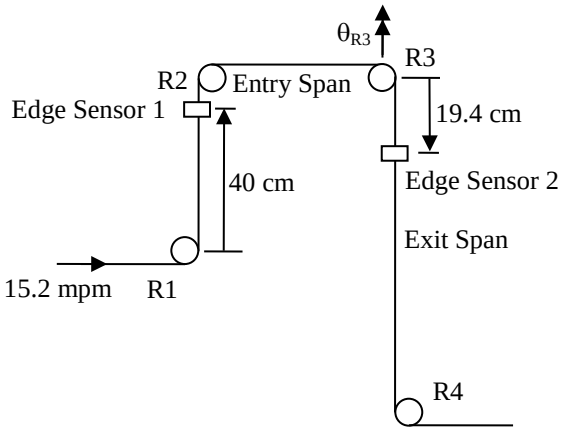

Figure 1 – Test Setup

As noted in Figure 1 web edge sensors were located in the pre-entry and exit spans. A sensor is placed in the exit span to capture the maximum lateral deformation of the web in the entry span. A sensor was placed in the pre-entry span to help determine when moment transfer begins. Lateral deformations will be shown in Figures 2 and 3 at average web stress levels of 14 and 37.2 MPa, respectively. One indication that moment transfer has occurred is when the lateral deformation in the pre-entry span deviates from zero. When moment transfer begins the lateral deformation in the entry span will decrease corresponding to the amount of lateral deformation in the pre-entry span. Straight lines have been plotted in Figures 2 and 3 to show what the lateral deformation would have been had no moment transfer occurred on roller R2. Any deviation of the lateral deformation data from the line is a second indication that moment transfer has occurred. Using these indicators moment transfer begins somewhere in the range (0.005-0.0067 rad) of misalignment in Figure 2 for an average web stress level of 14 MPa. In Figure 3 moment transfer begins somewhere in the range (0.015-0.0167 rad) of misalignment for an average web stress level of 37.2 MPa.

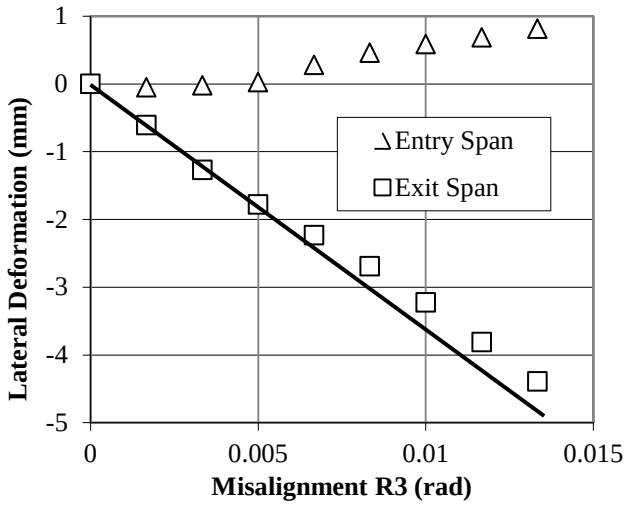

Figure 2 – Web lateral deformations at an average web stress of 14 MPa

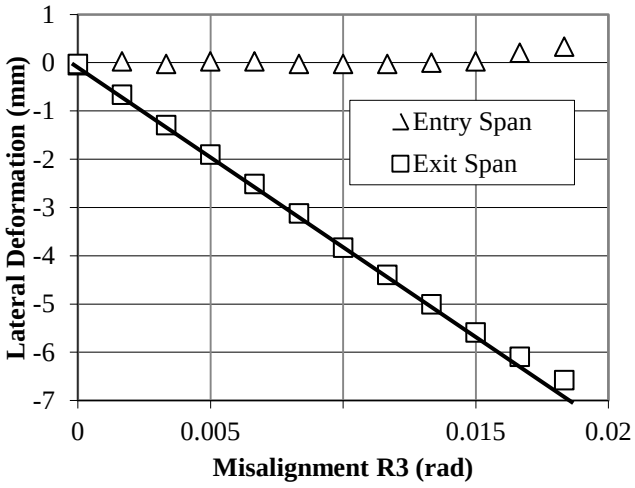

Figure 3 – Web lateral deformations at an average web stress of 37.2 MPa

The misalignment angles of roller R3 (θ_{R3}) required to induce web wrinkles at various average web stress levels are presented in Figure 4. The average web stress level is that due to web tension. The results show that the wrinkles were generated at the entry to the misaligned roller (R3) when the average web tensile stress was less than 20.7 MPa (3000 psi). At web tensile stresses greater than 20.7 MPa the wrinkles form at the entry of the upstream roller (R2). When the tensile stress becomes lower than 10.3 MPa (1500 psi), the misalignments required to induce wrinkles become large. This is due to the friction forces between the web and roller becoming too low to sustain a wrinkle at the CMD stress level predicted by the wrinkle failure criterion expression {1}. The combination of low tension with the fixed web velocity promotes air entrainment and decreases the apparent friction coefficient. This type of wrinkling has been previously

analyzed [10] and is not the focus of this study. Results from the use of single span theory [2] are shown in Figure 4. This theory appears to work well when the web tensile stress is less than 20.7 MPa (3000 psi) when compared to the test data in the 10.3 to 20.7 MPa tensile stress range where wrinkles were forming on roller R3. For cases where the web tensile stress exceeded 20.7 MPa the web wrinkles formed first on roller R2 and the test data deviate from the single span theory. The objective of this study is to investigate the wrinkling behaviors at web tensile stresses greater than 10.3 MPa in Figure 4 and determine why the wrinkles form on roller R3 at lower web tensile stresses but then initiate on roller R2 for higher web tensile stresses. Earlier using lateral deformation data it was found that moment transfer began in the range (0.005-0.0067 rad) of misalignment at a web stress of 14 MPa. When the average web stress level increased to 37.2 MPa moment transfer began in the range (0.015-0.0167 rad) of misalignment. The wrinkles that form at these stress levels in Figure 4 occur at yet higher misalignments than those required to initiate moment transfer. Thus moment transfer is present whether wrinkles are forming on roller R3 at lower web stress levels or on R2 at higher web stress levels.

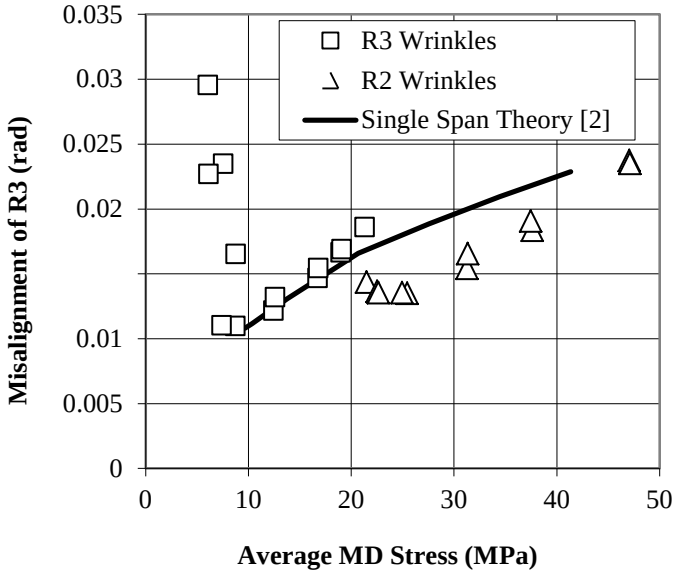

Figure 4 – Misalignments at roller R3 required to induce wrinkles on roller R2 and R3.

EXPLICIT SIMULATION OF WRINKLE DUE TO MOMENT TRANSFER

Moment transfer has been simulated previously [5] without consideration of wrinkling. Those simulations were validated by comparison of results to web edge deflections and internal moments that were measured in the laboratory. In the present study, further simulations will be conducted to study wrinkle formation in cases where moment transfer exists. Similar to the previous moment transfer study [5], a multi-span model is created as shown in Figure 5 but now used to simulate wrinkle formation. The contact friction forces between the web and roller will be studied to investigate the CMD stress distribution on R2. The experimental results, such as lateral displacements and critical angles, will be compared to simulation results to validate the FE model. The

wrinkle failure criterion developed previously will be validated using simulation and experimental results as well.

Finite Element Model Setup

Abaqus/Explicit was used to model the experimental setup shown in Figure 1 and described in the section on Experimental Procedure and Results. The simulations will be conducted for two average web tension stress levels, 13.8 MPa (2000 psi) and 37.2 MPa (5400 psi). These tensile stress levels were chosen because the lower level produced wrinkling on roller R3 during tests while the higher level produced wrinkles on roller R3. The test results from Figure 4 show that 12.9 mrad of misalignment of R3 was required to produce a wrinkle on R3 at 13.8 MPa of web tension. At a web tension of 37.2 MPa, 18.3 mrads of misalignment was required at R3 to produce a wrinkle on R2. In the simulations, R3 was misaligned while web tension was maintained constant to induce moment interaction between spans. Analytical rigid rollers and shell (S4R) elements were used to model the web in these simulations.

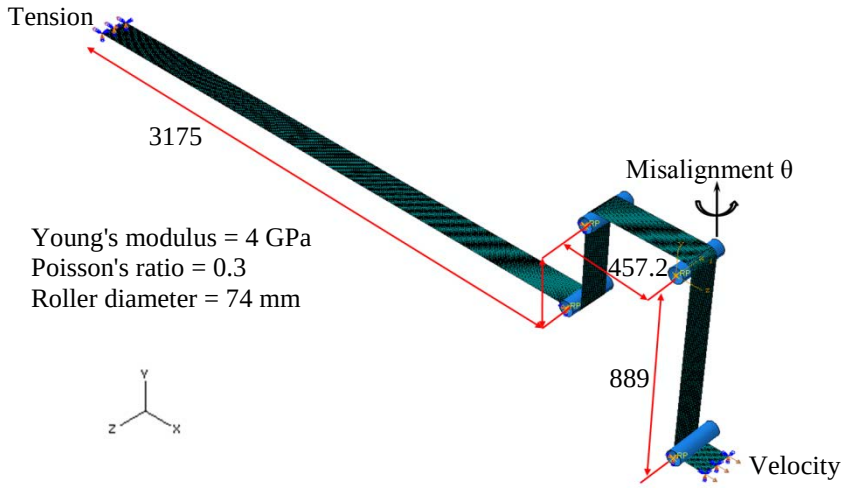

Figure 5 – A four-roller FE model setup for wrinkle formation during moment interaction. (Length unit: mm)

The mission of the experiments was to investigate wrinkling due to moment transfer caused by downstream roller misalignment. Thus bare aluminum rollers were used in the R2 and R3 roller locations in the experiments. Under static conditions a coefficient of friction of 0.3 would be common between the bare aluminum and the polyester web. For a moving web, air entrainment reduces the web friction coefficient depending on web velocity, web tension, the viscosity of air and the surface roughness of the web and rollers. The friction coefficients were measured for the two web tension levels that will be simulated during the testing. The measured friction coefficient between roller R2 and the polyester web was 0.13 for a web stress of 13.8 MPa and a web velocity of 15.2 mpm. When the web stress was increased to 37.2 MPa, with the web velocity still at 15.2 mpm, the friction coefficient between R2 and the polyester increased to 0.23. The friction coefficient for roller R3 was measured at 0.28 at both web tension levels. The larger surface roughness of roller R3 (compared to R2) was responsible for producing the larger friction coefficient. The friction coefficients of rollers R1 and R4 were set to unity in the

simulations because of the high friction coating described earlier in the Experimental Procedure. A mesh size of 6.35 mm square (0.25 inches square) was shown to provide convergence of the output stresses from the simulations. Both the lateral deformations and the misalignments required to produce wrinkles measured during tests will be used to validate the results of the simulations. The analysis of moment transfer behavior on R2 will be studied at first, and the comparison between simulations and experiments and discussion of wrinkle formation will follow.

Analysis of Moment Transfer Behavior on R2

To investigate the moment transfer behavior on roller R2, several simulations were conducted with various misalignment angles for an average web stress level of 13.8 MPa. Five misalignment angles were simulated including 1, 5, 7, 10 and 12.9 mrads. The internal moment values in the web for the simulations are shown in Figure 6. These moments were estimated using the steady state machine direction (MD) stresses from the simulations at MD locations using following expression:

$$M = \int \sigma_{MD} z dA \approx \sum_{i=1}^{n} \sigma_{MDi} z_i A_i \qquad \{6\}$$

where σ_{MDi}, z_i and A_i are the MD stress levels at the nodes, the distances between the nodes and the elastic axis and the cross sectional area of the web associated with the nodes, respectively. The vertical lines indicate the locations of rollers R1, R2 and R3. The moment reaches its peak value at the exit of R2 and then decreases almost linearly as the web approaches R2 in the entering span. Eventually, the moment decreases to zero when the web arrives at the misaligned roller R3 and is consistently zero on the roller until the web exits R3. In Figure 6 moment transfer over R2 became evident for a misalignment angle of 5 mrads. This is consistent with the test results shown in Figure 2. The moments at R2 entry and exit for different misalignments of R3 are shown in Figure 7. Closed form analyses of moment transfer [4] rely upon an estimate of a critical moment that can be resisted by friction at R2:

$$M_r = \frac{\mu \pi T_w t W^2}{8} \qquad \{7\}$$

where μ is the friction coefficient, T_w is the average web stress due to tension and W is the web width. For the given test parameters this moment is calculated as 38.2 N-cm (3.31 in-lb). Once moment transfer begins the critical moment can be calculated from the simulations from the difference of the moments between the exit and the entry of R2. This difference of moment is shown in Figure 7 and is consistent with the moment given by expression {7}. As the misalignment angle increases, the difference in moment between R2 exit and entry (M_r) decreases slightly which is not predicted by expression {7}.

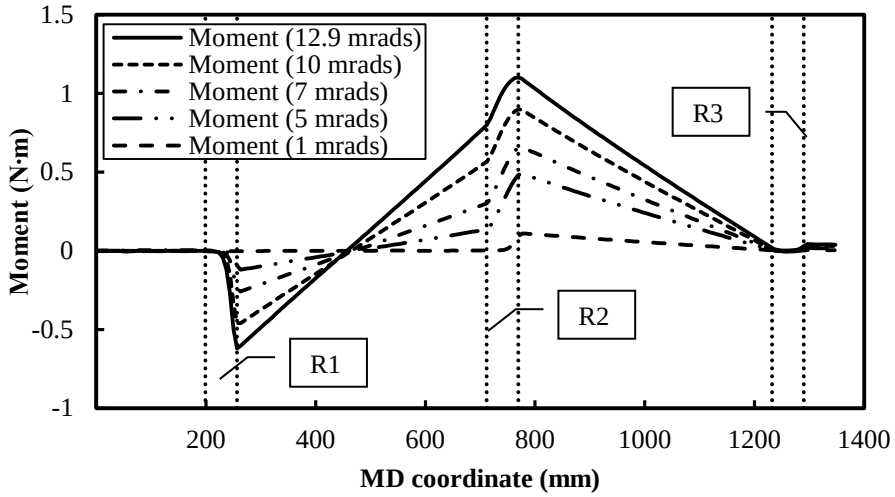

Figure 6 – The moment distribution in the web as affected by the misalignment of roller R3, T_w=13.8 MPa.

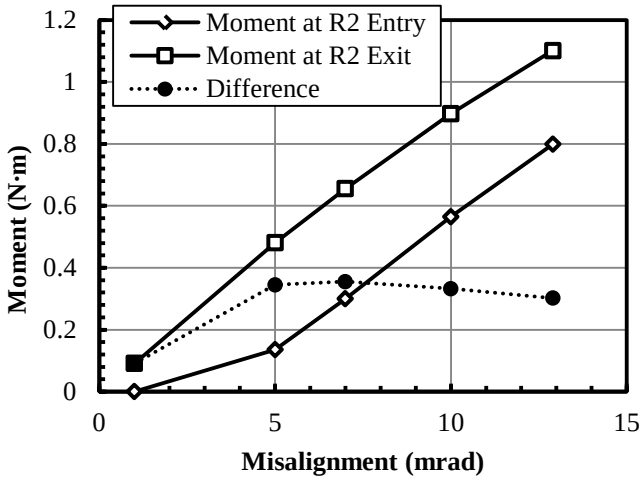

Figure 7 – Moments at entry and exit of roller R2, T_w=13.8 MPa.

Vector plots of contact shear force were used to reveal the frictional force distribution on R2 in [5] to develop a more accurate expression than expression {7} to predict the moment that can be resisted by friction on R2. These vector plots show the direction and magnitude of contact shear forces at nodes between the web and the surface of roller R2. The size of vector symbol implies the magnitude of contact shear force. In Figure 8, the contact shear forces are presented in such vector plots for the misalignments simulated. The contact shear force is the force applied on the web which is caused by the contact frictional force between roller and web. When the downstream misalignment is small, for instance, 1 mrads in Figure 8 (a), the contact shear forces on R2 are aligned with the machine direction but exist only near the exit of R2. This is consistent with Figures 2 and 6 which show that moment transfer has not begun for a misalignment of 1

mrad at R3. After moment transfer begins, the contact shear forces on R2 become more complicated as shown in Figures 8 (b) to (e). Note that the center of rotation of the friction force vectors move as the misalignment angle increases. From Figures 8 (a) to (e), the center of rotation on R2 moves from R2 exit to R2 entry. Also note the center of rotation begins near the CMD web center in Figure 8(a) and proceeds near the web edge in Figure 8(e).

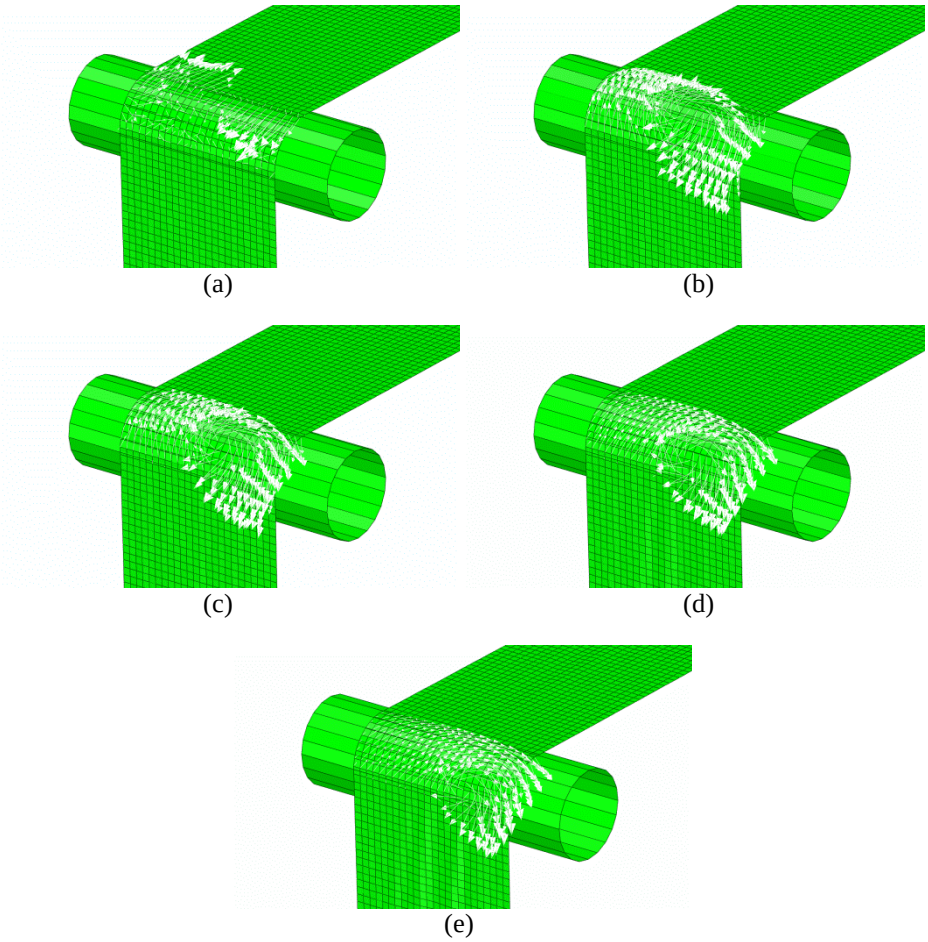

Figure 8 - Vector plot of contact shear force distribution on R2, T_w=13.8 MPa: (a) θ = 1 mrads; (b) θ = 5 mrads; (c) θ = 7 mrads; (d) θ = 10 mrads; (e) θ = 12.9 mrads.

The distribution of the friction force vectors affect the CMD stress distribution on R2 which is shown in Figure 9. There are two CMD stress behaviors evident. The first behavior is shown in Figures 9 (a) to (c); the CMD stresses on R2 are all compressive but they have not surpassed the critical stress calculated by Timoshenko's buckling equation expression {1} and hence wrinkles are not produced. The second behavior is witnessed in Figures 9 (d) and (e); here the CMD stresses at the entry to R2 are compressive and surpass Timoshenko's critical stress. Based upon the wrinkle failure criterion developed, wrinkles are attempting to form near the entry of R2. Friction forces and slippage of the web on the roller result in CMD tensile stress on the roller which prevents wrinkles from

forming and transiting the roller R2. This is consistent with the data presented in Figure 4 in which wrinkles did not form on R2 at this average web tensile stress (13.8 MPa).

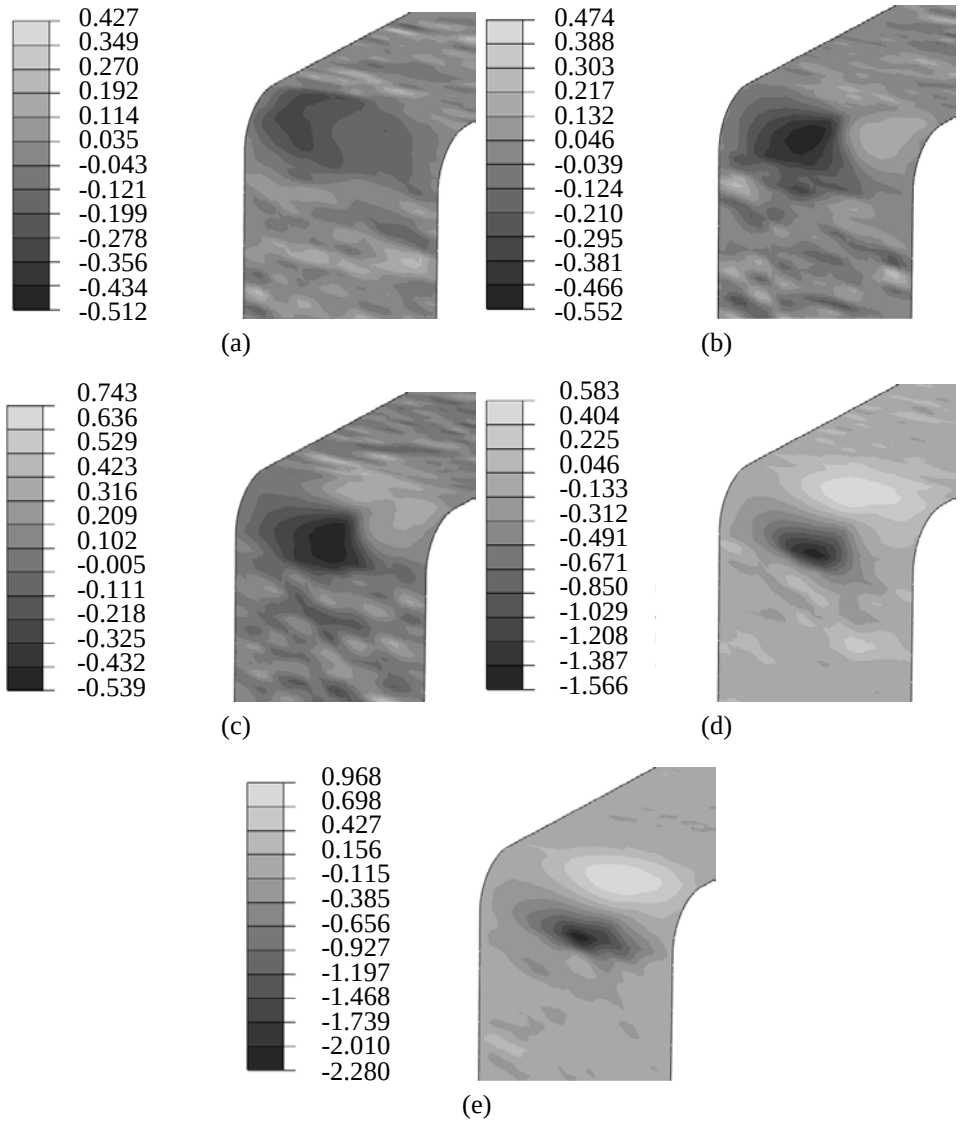

Figure 9 – CMD stress distribution on R2, T_w=13.8 MPa: (a) θ = 1 mrads; (b) θ = 5 mrads; (c) θ = 7 mrads; (d) θ = 10 mrads; (e) θ = 12.9 mrads. (Stress unit: MPa)

Comparison of Lateral Deformations: Simulations versus Tests

During the tests lateral deformations were measured at several locations in addition to those shown in Figure 1. The locations of all sensors are shown in Figure 10.

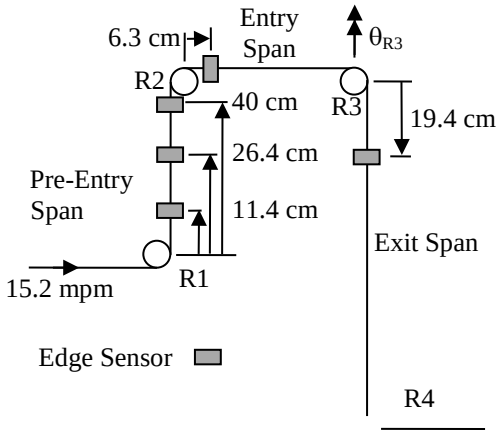

Figure 10 – Edge Sensor Locations

The lateral deformations are shown in Figures 11 (a) and (b) for the simulations and tests conducted at a web tensile stress of 13.8 MPa coupled with a misalignment of 12.9 mrads and for web tensile stress of 13.8 MPa coupled with a misalignment of 18.3 mrads. Note that in general the measured lateral deformations agree nicely with the steady state deformations predicted by the simulations. The slope extracted from the simulations show the web is entering R3 precisely at the set misalignments. Thus normal entry to roller R3 is being achieved.

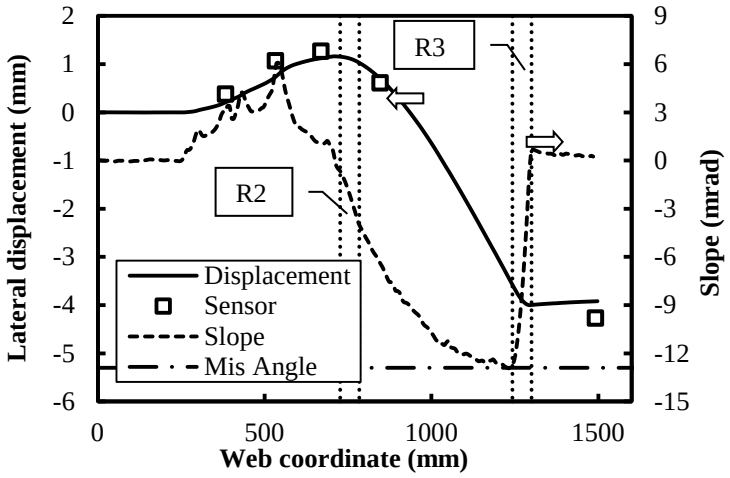

(a)

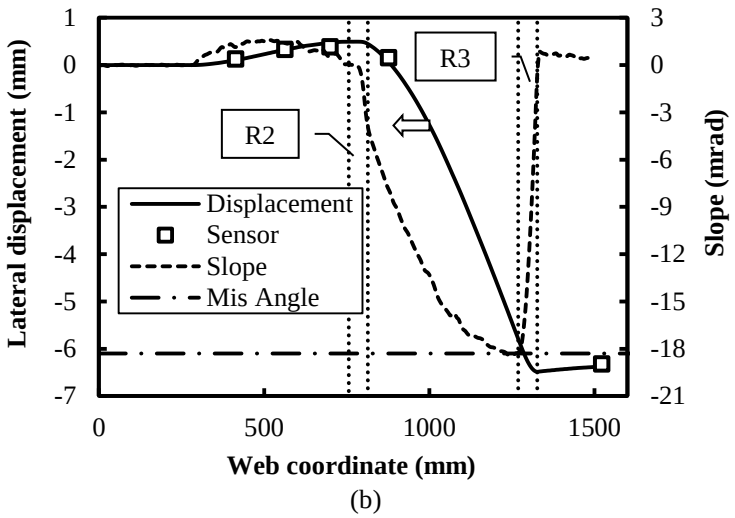

(b)

Figure 11 – Lateral displacement and slope comparison: (a) T_w=13.8 MPa and θ_{R3}=12.9 mrads; (b) T_w=37.2 MPa and θ_{R3}=18.3 mrads.

The slopes were extracted using a finite difference approximation on the lateral deformations output from the simulations. The slopes at the entry to R2 are also close to zero but it is also obvious the slope of the web has become non-zero prior to exiting R2, even more so for the low web tension case. The slopes witnessed at R2 and R3 are consistent with previous investigations of moment transfer [4, 5]. Based on the good agreement between the simulated and tested lateral deformations and that the slopes demonstrated normal entry to rollers R2 and R3 the simulations are proven to be a valid representation of the tests conducted in the laboratory.

The Development of CMD Compressive Stresses in the Web on R2

The calculated internal moments for 13.8 and 37.2 MPa web stress levels for misalignments that induced wrinkles are shown in Figures 12 (a) and (b), respectively. The internal moments were calculated using expression {6}. Moment is being transferred from the entering span to the pre-entering span in both cases. From the lateral deformations presented in Figures 2, 3 and 11 this was already confirmed. The levels of moment transfer are very different for the two cases. For the low tension case, the moment transferred to pre-entering span is greater than the high tension case. The greater moment transferred to the pre-entry span combined with lower web tension induced greater lateral deformation in the pre-entry span in Figure 11 (a) compared to Figure 11 (b). Note that a much greater moment is absorbed in friction between the web and R2 for the high tension case shown in Figure 12 (b) compared to the low tension case in Figure 12 (a). Based on expression {7} this should be expected given the friction coefficient increases from 0.13 to 0.23 combined with the web tension increase from 13.8 to 37.2 MPa. This will result in greater frictional contact forces between the web and roller R2 when moment transfer is occurring that will impact the CMD stresses.

In Figure 8 the center of rotation of the frictional forces moved from the exit to the entry of R2 with increased misalignment of R3. The wrinkle formed on R3 at 12.9 mrads for the low tension case and moment transfer was estimated to have begun in Figure 2 in

the range of 5 to 6.7 mrads. When the wrinkle formed on R3 moment transfer across R2 was fully developed. The friction contact forces between the web and R2 are shown in Figure 13 for a web tension of 37.2 MPa and a misalignment of R3 of 18.3 mrads. Note the center of rotation of the friction forces is approximately half way between the exit and the exit. From Figure 3 it was estimated that moment transfer began for the high tension case in the range of 15 to 16.7 mrads of misalignment at R3. Thus when the wrinkle developed on R2 at 18.3 mrads of misalignment, moment transfer had recently begun.

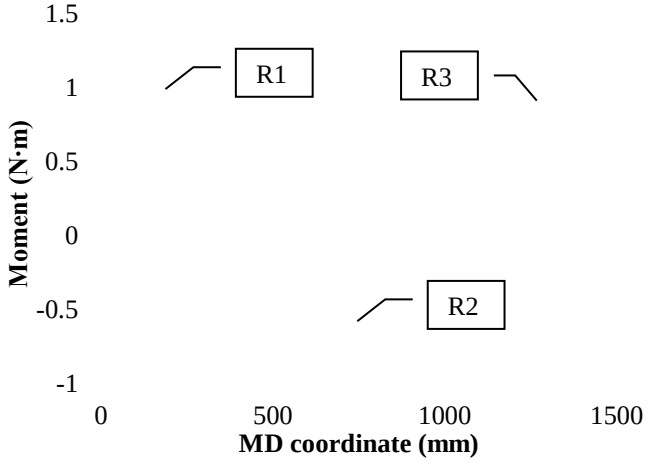

(a)

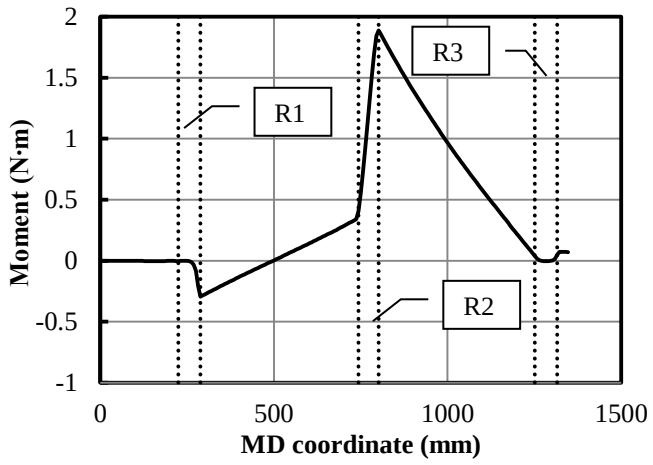

(b)

Figure 12 – Calculated moments for each tension: (a) T_w=13.8 MPa and θ_{R3}=12.9 mrads; (b) T_w=37.2 MPa and θ_{R3}=18.3 mrads.

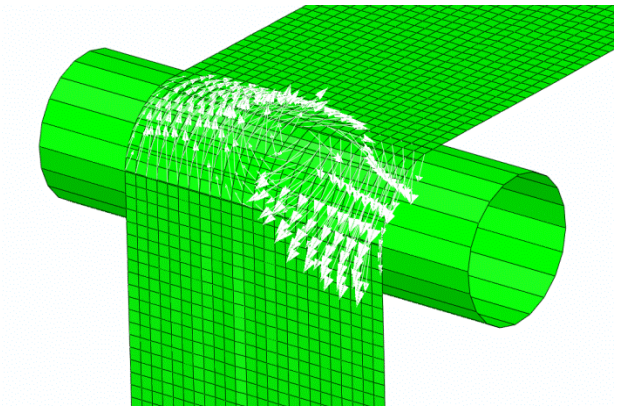

Figure 13 - Vector plot of contact shear force distribution on R2, T_w=37.2 MPa and θ_{R3}=18.3 mrads.

For the low tension case (T_w=13.8 MPa) the CMD stresses on R2 were smaller than the wrinkle failure criterion and wrinkles were observed on R3 in Figure 4. The center of rotation of frictional forces is near the entry to R2, as shown in Figure 8 (e). The CMD friction forces near the entry of R2 will generate the CMD compressive stresses at the entry of R2 in the web seen in Figure 9 (e) (note the CMD components of the forces oppose one another in Figure 8(e)). As the web nears the exit of R2, the CMD components of the friction forces in the web are in one direction resisting lateral slippage since the web is rotating about the entry location to R2. This results in the tensile CMD stress observed in the web in and before the exit of the web from R2 in Figure 9 (e).

For the high tension case (T_w=37.2 MPa) wrinkles were observed on R2 for a misalignment of 18.3 mrads in Figure 4. The CMD components of the frictional forces in Figure 13 all point to the left side of the web. The misalignment of R3 is steering the web to the left in the entry span. The bending moment in the web resulting from this steering produces higher MD stress on the right half of the web compared to the left half. These stresses produce higher normal contact pressures on the right half of the web in comparison to the left half. Note the magnitudes of the vectors of contact shear force are in fact larger on the right half of the web in comparison to the left half. The CMD components of the contact shear forces must be reacted internally in the web in the form of CMD compressive stress.

This demonstrates the necessity of using the explicit method to study the frictional forces due to moment transfer. These frictional forces are responsible for the CMD stresses observed in the web transiting R2. In the Introduction there was discussion that a disturbance is required to produce the CMD stresses that induce wrinkles on rollers. Roller misalignment is the primary disturbance in this case. When moment transfer is prevented the disturbance produces trough instabilities in the entry span which in turn produce negative CMD stresses to form on the misaligned roller. The troughs are responsible for the negative CMD stress on the downstream roller because they decrease the projected width of the web in the entry span. The projected web width increases as the web enters the misaligned roller and the trough amplitude vanishes. To establish the magnitude of the negative CMD stresses required nonlinear finite element analysis [2]. When moment transfer is allowed, both troughs and frictional contact forces of the form shown in Figures 8 (e) and 13 result from the misalignment disturbance. Both the troughs and these frictional forces can cause negative CMD stresses to form on R2 and R3. Note

in Figures 8 (d) and (e) that the explicit method captures both the trough instability (visible in the pre-entry span) and the frictional forces of contact.

The Development of Wrinkles on Rollers R2 and R3

Figures 14 (a) and (b) show the CMD stress distributions on R3 and R2, respectively, for the low tension (13.8 MPa) case. Note the charts of CMD stresses along the centerline of web which accompany Figures 14 (a) and (b). The vertical lines indicate where the web enters and exits rollers. From the contour plots and the charts, the CMD stresses are shown to be negative and distributed uniformly on R3. The stresses on R2 begin negative but quickly become positive as the web moves across the roller. In tests it is common to observe small wrinkles near at the entry of R2 which do not transit R2. In this case it is obvious that the wrinkles will preferentially form on R3, initiating at the entry and continuing to near the exit. The negative CMD stresses from the simulations surpass the critical buckling stress of -1.53 MPa (-222 psi) over the majority of the roller R3.

Figures 14 (c) and (d) show the CMD stress distributions on R3 and R2, respectively, for the high tension (37.2 MPa) case. In Figure 14 (c) the negative CMD stresses on R3 are roughly half of the critical stress, thus no wrinkles would be expected on R3. In Figure 14 (d) the negative CMD stresses surpass the critical buckling stress from the entry to about half the wrap of the web about R2. Thus wrinkles would be expected over the first half of R2.

These observations are consistent with the test results presented in Figure 4.

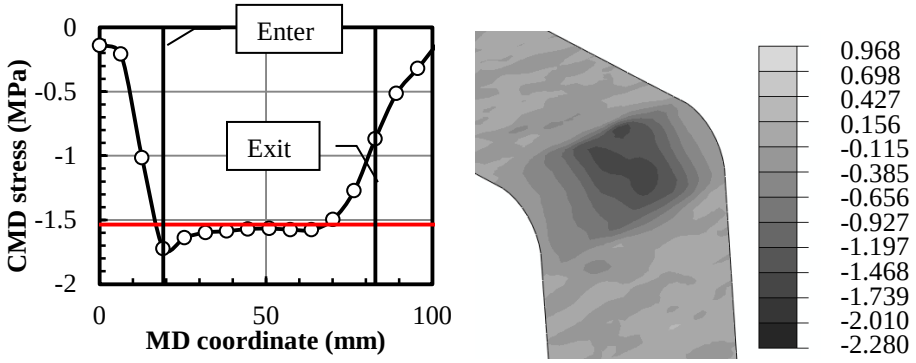

(a)

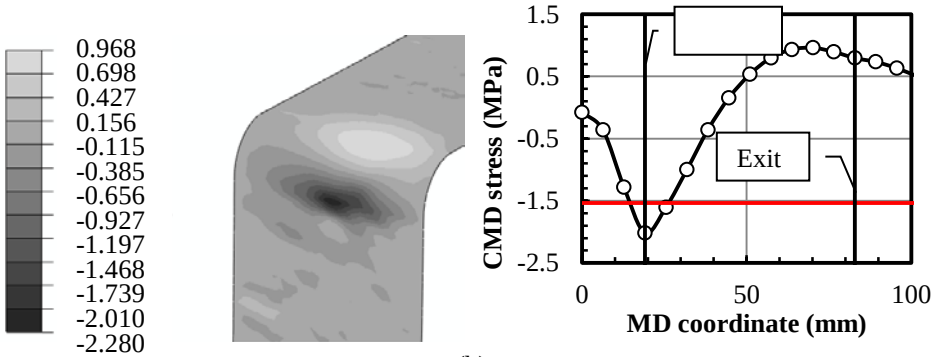

(b)

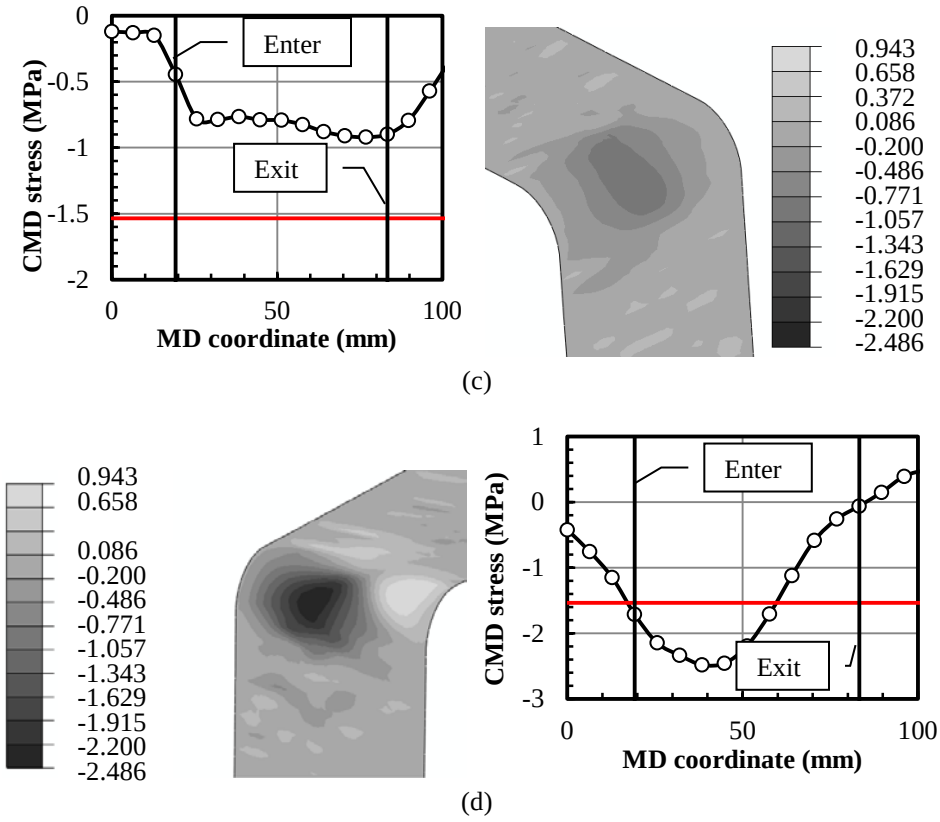

Figure 14 – CMD stress contours in the web and CMD stress distributions in the MD direction on the web centerline: (a) T_w=13.8 MPa and θ_{R3}=12.9 mrads, R3 view; (b) T_w=13.8 MPa and θ_{R3}=12.9 mrads, R2 view; (c) T_w=37.2 MPa and θ_{R3}=18.3 mrads, R3 view; (d) T_w=37.2 MPa and θ_{R3}=18.3 mrads, R2 view. (Stress unit: MPa)

These simulations shown thus far were run with a 45.7 cm (18 in) pre-entry span length. Other simulations were conducted with an 81.3 cm (32 in) pre-entry span length as tests were run for this configuration as well. The test data is superposed on the test data from Figure 4 as well as results from the single span theory [2] in Figure 15. Note per tests the effect of a different pre-entry span length is not detectable. The simulations were conducted at the two tensions of 13.8 and 37.2 MPa again. When the web tension was 13.8 MPa a misalignment of 13.5 mrads produced a wrinkle on R3 per the failure criterion. When the web tension was 37.2 MPa a misalignment of 18.3 mrads produced a wrinkle on R2 per the failure criterion. Both the tests and the simulations are consistent in showing that the pre-entry span length has little consequence on the wrinkling behavior. This is also consistent with moment transfer theory since the moment at the exit of R2 is mainly related to the length of the entering span [4].

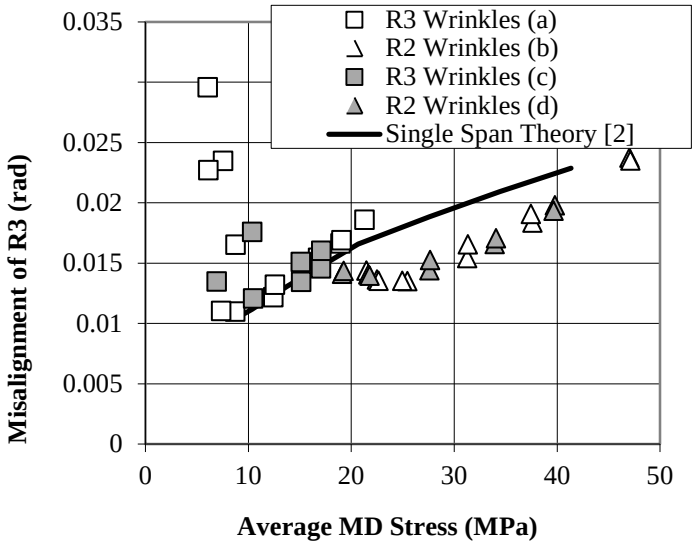

Figure 15 - Misalignments at roller R3 required to induce wrinkles on roller R2 and R3: (a) R3 Wrinkles, Pre-entry Span Length 45.7 cm; (b) R2 Wrinkles, Pre-entry Span Length 45.7 cm; (c) R3 Wrinkles, Pre-entry Span Length 81.3 cm; (d) R2 Wrinkles, Pre-entry Span Length 81.3 cm.

CONCLUSIONS

These analyses have shown the level of computation and simulation that is required to model wrinkling when moment transfer is occurring. The argument could be presented that it is easier to limit the misalignment which caused the wrinkling and the moment transfer than it is to perform the simulations. It was shown that the single span theory was applicable for the low tension domain where wrinkles form on roller R3 [2]. When is the single span theory applicable and when is it not? Simulations of the complexity shown here would be required to answer this question. A benefit of this work is that through the frictional force distributions such as those shown in Figures 8 and 13 that insight is gained with regard to the development of CMD stresses on roller R2. In all analysis there may be limits due to other behaviors, a slack edge for instance. A web entering slack edge behavior will behave differently with regard to wrinkling than a taut web and that behavior has not been studied herein. Can we forecast what behaviors in wrinkling will occur at web tensions higher than that shown in Figures 4 and 15? Is it possible that wrinkles could again form on R3 at some higher web tension? The methods and simulations developed herein give us tools where such unknowns can be explored.

ACKNOWLEDGEMENTS

The authors would like to thank the industrial sponsors of Web Handling Research Center at Oklahoma State University for providing the funding which made this study possible. The test results shown in this work were acquired in June of 1997 at the Corporate Research Labs of 3M Company. The efforts of Doug Kedl, Ron Swanson, Jim Dobbs, Dan Carlson, John Huzinga and Tim Walker were greatly appreciated. Keith Good was allowed the privilege of being part of, to our knowledge, this first investigation

of wrinkling in multiple web spans. He is grateful to those at 3M Company who made this possible. The edge detectors used in this research to detect edge deformation were an internal development of 3M Company. The accuracy of these detectors was ±25 μm (±0.001 in).

REFERENCES

1. Gehlbach, L. S., Good, J. K. and Kedl, D. M., "Prediction of Shear Wrinkles in Web Spans," TAPPI Journal, Vol. 72, No. 8, August 1989.
2. Beisel, J. A. and Good, J. K., "The Instability of Webs in Transport," ASME Journal of Applied Mechanics, Vol. 78, No. 1, January, 2011, pp. 1-7.
3. Yurtcu, H. Y., Beisel, J. A. and Good, J. K., "The Effect of Roller Taper on Webs," TAPPI Journal, Vol. 11, No. 11, November 2012, pp. 31-38.
4. Good, J. K., "Shear in Multi Span Web Systems," Proceedings of the Fourth International Conference on Web Handling, Web Handling Research Center, Stillwater, Oklahoma, June, 1997.
5. Fu, B., Reddy, A., Vaijapurkar, S., Markum, R. and Good, J. K., "Boundary Conditions that Govern the Later Mechanics of Flexible Webs in Roll to Roll Process Machines," ASME Journal of Computational and Nonlinear Dynamics, accepted for publication 2013.
6. Abaqus Analysis User's Manual, Section 25.1, 2012.
7. Good, J. K. and Straughan, P., "Wrinkling of Webs due to Twist," Proceedings of the Fifth International Conference on Web Handling, Web Handling Research Center, Stillwater, Oklahoma, June, 1999.
8. Timoshenko, S. P. and Gere, J. M., Theory of Elastic Stability, 1st Ed. McGraw-Hill, New York, 1987.
9. Kyriakides, S. and Corona, E., Mechanics of Offshore Pipelines Vol.1 Buckling and Collapse, 1st Ed., Elsevier, 2007.
10. Good, J. K. and Beisel, J. A., "Calculations Relating to Web Buckling resulting from Roller Misalignment", TAPPI Journal, December, 2006, pp. 9-16.